Successive homoclinic doublings bifurcations from orbit-flip

Motomasa Komuro （小室元政）
Department of Mathematics
The Nishi-Tokyo University
2525 Yatsusawa, Uenohara-mati
Yamanashi 409-01, Japan

Collaboration with

Hiroshi Kokubu
Department of Mathematics
Faculty of Science
Kyoto University
Kyoto 606-01, Japan
kokubu@kusm.kyoto-u.ac.jp

and

Hiroe Oka
Department of Applied Mathematics and Informatics
Faculty of Science and Technology
Ryukoku University
Seta, Otsu 520-21, Japan
oka@rins.ryukoku.ac.jp

October 29, 1995

1 Introduction

Motivation Extensive study has recently been made for bifurcations occurring in a neighborhood of a codimension two homoclinic orbit in a three-dimensional vector field, and in particular, it became known that some types of codimension two homoclinic orbits which are bi-asymptotic to hyperbolic equilibria with real principal eigenvalues can give rise to multiple homoclinic orbits; an N-times rounding homoclinic orbit arises under perturbation in a tubular neighborhood of the unperturbed orbit where N being an integer ([27], [1], [11, 12], [25], [7]). Such a homoclinic orbit is referred to as an N-*homoclinic orbit* with respect to the original unperturbed one. The bifurcation of such multiple homoclinic orbits are, however, still far from being understood. For instance, when one varies the eigenvalues of the equilibria it has been observed by a numerical simulation a very complicated bifurcation involving many such multiple homoclinic orbits. See, for instance, Figure 4.1 and [10].

The purpose of this and forthcoming papers is to obtain a better understanding of such complicated bifurcations for multiple homoclinic orbits by combining results from homoclinic bifurcation analyses with those from numerical experiments. To be more precise, we shall take one particular type of codimension two homoclinic orbits with real eigenvalues in $\mathbb{R}^3$, called *orbit-flip*, and study its bifurcation of multiple homoclinic orbits appearing in a tubular neighborhood of the original orbit-flip. The main interest of the present paper lies in the occurrence of *successive homoclinic doubling* bifurcations under an appropriate condition, which is a part of the total bifurcations for multiple homoclinic orbits. Here the homoclinic doubling bifurcation refers to the bifurcation of a homoclinic orbit changing into a twice rounding homoclinic orbit in a tubular neighborhood of the original one. The homoclinic doubling bifurcation associated to real principal eigenvalues was first studied by Yanagida[27] where he asserted that there are three kinds of codimension two homoclinic orbits that can undergo the homoclinic doubling bifurcations: these are now called (i) a homoclinic orbit with resonances, (ii) that of inclination-flip type, and (iii) that of orbit-flip type. See [1], [11, 12] and [25] for efforts toward justifying and generalizing Yanagida's original ideas concerning these three types of homoclinic doubling bifurcations. In this paper, we shall show the existence of cascade of homoclinic bifurcations starting from a homoclinic orbit of orbit-flip type followed by those of inclination-flip type. Relation between such a global bifurcation and a local bifurcation from orbit-flip will also be discussed in the last section.

Continuous piecewise-linear vector fields Since the cascade of homoclinic doublings is a totally global bifurcation, we need an aid of numerical experiments in which we must choose a concrete set of ordinary differential equations that exhibits the desired bifurcation. In this paper we employ a family of *continuous piecewise-linear vector fields* for such a model equation. The advantage of using such continuous piecewise-linear vector fields is that, firstly it is easier to analyze dynamics and bifurcations of the vector fields because of their piecewise-linearity, and secondly, according to a general theory established by the second author of this paper ([14]), we can obtain a kind of normal forms for generic continuous piecewise-linear vector fields if one specifies the number of regions on which the vector field is linear, and the normal form is completely characterized in the sense of linear conjugacy in terms of the eigenvalues at equilibria in each of these linear regions. This means that these eigenvalues are considered to be the bifurcation parameters of the normal form equations, which is suitable for our purpose of this and subsequent papers. In our case, we use the normal form of piecewise-linear vector fields with two linear regions in $\mathbb{R}^3$, and hence it possesses six parameters in total. Moreover it is easy to derive an explicit condition in terms of the eigenvalue parameters for the existence of orbit-flip homoclinic orbits. Using this information, we can set up the model problem in a tractable way and perform very precise numerical experiments based on explicitly computed analytic formulas. The results obtained by such analyses and experiments will also be valid for general smooth vector fields, because the homoclinic bifurcation theory only uses information from the return map along the original homoclinic orbit and hence the piecewise-linearity does not lose essential information for it is constructed in the same way as in the smooth case.

Main results Using such a family of continuous piecewise-linear vector fields, we shall demonstrate the presence of the following global bifurcations in this paper: Since the original homoclinic orbit is assumed to be of orbit-flip type, it undergoes the first homoclinic doubling bifurcation and gives rise to a 2-homoclinic orbit. It then turns to be a homoclinic orbit of inclination-flip type after a slight change of parameters and thus undergoes the second doubling bifurcation creating a 4-homoclinic orbit. This 4-homoclinic orbit becomes again that of inclination-flip type for a further variation of parameters and we find 8-homoclinic orbit through the third homoclinic doubling bifurcation. By numerical experiments for our family of continuous piecewise-linear vector fields we can similarly see that each 2^k-homoclinic orbit becomes that of inclination-flip type and gives rise to a 2^{k+1}-homoclinic orbit through the homoclinic doubling bifurcation. In fact we have observed up to $2^6 = 64$-homoclinic orbits through

these doubling bifurcations. Such precise numerical experiments could only be done by using piecewise-linear vector fields, since it is in general hard to find a homoclinic orbit as an intersection of the stable and unstable manifolds, but for piecewise-linear vector fields, those manifolds are locally given by a straight line or a plane and hence it is quite easy to find a parameter value where an orbit precisely lies on these manifolds.

In order to explain this bifurcation more theoretically, we derive a two-parameter family of unimodal maps as singular limit of the Poincaré maps along homoclinic orbits. We locate bifurcation curves for this family of unimodal maps in the two-dimensional parameter space and these curves basically agree with those for the piecewise-linear vector fields. In particular, we show, using a standard technique from the theory of unimodal maps (see e.g. [2], [18], [19]), that there exists an infinite cascade of doubling bifurcations which corresponds to the sequence of homoclinic doubling bifurcations for the piecewise-linear vector fields described above. Since our unimodal map has a singularity at a boundary point of its domain of definition, the doubling bifurcation is slightly different from that for standard quadratic unimodal maps, for instance the Feigenbaum constant associated to accumulation of the doubling bifurcations is different from the standard value 4.6692.... Basic qualitative similarity between the bifurcations of our unimodal map family and the piecewise-linear vector fields strongly suggest that there does also exist a cascade of homoclinic doubling bifurcations in our family of continuous piecewise-linear vector fields in a way described by their singular limit unimodal maps.

2 Preliminaries

Consider a family of vector fields X_η on $\mathbb{R}^3$ with a hyperbolic equilibrium point O and suppose that it admits a homoclinic orbit Γ to the equilibrium point for $\eta = 0$ where the linearization matrix possesses eigenvalues λ_u and $-\lambda_{ss}$, $-\lambda_s$ with $-\lambda_{ss} < -\lambda_s < 0 < \lambda_u$. The eigenvalues λ_u and $-\lambda_s$ are called principal. Then for sufficiently small η, X_η may possess a homoclinic orbit rounding twice in a small tubular neighborhood of the original homoclinic orbit. Such a bifurcation is referred to as *homoclinic doubling bifurcation* and the bifurcating homoclinic orbit is called a doubled homoclinic orbit or a 2-homoclinic orbit with respect to the original one which is called the primary or 1-homoclinic orbit.

For the homoclinic orbit, we can generically expect the following two conditions to be satisfied:

(Ev) $\lambda_u \neq \lambda_s$;

(Asy) Γ is tangent at O to the eigendirection associated to $-\lambda_s$ as t tends to $+\infty$.

Besides the stable manifold denoted by $W^s(O)$, we can consider another invariant manifold which is tangent to the eigendirections associated with λ_u and $-\lambda_s$. In this paper we call it an *extended unstable manifold* which we denote by $W^{eu}(O)$. Notice that the homoclinic orbit Γ is contained in $W^{eu}(O) \cap W^s(O)$. Generically we have

(Tr) $W^{eu}(O)$ and $W^s(O)$ intersect transversely along Γ.

A degenerate homoclinic orbit arises by breaking one of these genericity conditions, as in the following way.

Definition 2.1. Let Γ be a homoclinic orbit of the vector field $X = X_0$.

(Inc) Γ is called a *homoclinic orbit of inclination-flip type*, if (Ev) and (Asy) hold, but (Tr) does not, namely, $W^s(O)$ and $W^{eu}(O)$ are tangent along Γ;

(Orb) Γ is called a *homoclinic orbit of orbit-flip type*, if (Tr) and (Ev) hold, but (Asy) does not, namely, Γ lies in the strong stable manifold $W^{ss}(O)$;

(Res) Γ is called a *homoclinic orbit with resonance*, if (Tr) and (Asy) hold, but (Ev) does not, namely, the resonance condition $\lambda_u = \lambda_s$ is satisfied.

Remark 2.2. The proof of the center manifold theorem works as well for the existence of the extended unstable manifold $W^{eu}(O)$. See [8] for the proof. This invariant manifold is not unique, but has the unique tangent space along the homoclinic orbit, and hence the condition (Inc), which is sometimes referred to as the strong inclination property ([3]), is independent of the choice of the extended unstable manifold.

Bifurcations to doubled homoclinic orbits were first studied in [5] in the case of the Shil'nikov-type homoclinic orbit, together with the non-existence of the homoclinic doubling bifurcation for homoclinic orbits with real principal eigenvalues under the generic conditions (Asy), (Tr) and (Ev). Yanagida [27] then claimed that there are the above three possibilities of more degenerate homoclinic orbits with real principal eigenvalues that can generate a doubled

homoclinic orbit under perturbation. Since [27], a lot of work has been carried out toward completing and generalizing Yanagida's original ideas.

It was shown in [1] that the period-doubling bifurcation or the saddle-node bifurcation for a periodic orbit occurs in a generic two-parameter unfolding of a homoclinic orbit with resonant eigenvalues, depending whether the homoclinic orbit is twisted or non-twisted. Similar bifurcations are also shown for inclination-flip homoclinic orbits ([11, 12]) with the ratio $\nu = \frac{\lambda_s}{\lambda_u}$ of the principal eigenvalues satisfying $\frac{1}{2} < \nu < 1$. On the other hand, if the ratio ν is smaller than $\frac{1}{2}$, more complicated dynamics such as the shift dynamics accompanied by rich bifurcation phenomena in their creation possibly appear ([4], [7]). In particular, Homburg, Kokubu and Krupa [7] proved the existence of suspension of the Smale's horseshoe in unfoldings of an inclination-flip homoclinic orbit with $\nu < \frac{1}{2}$, $2\nu < \mu = \frac{\lambda_{ss}}{\lambda_u}$ and described how N-homoclinic orbits are created and destroyed in the unfolding. Sandstede [26] showed the existence of a shift dynamics in the unfolding of an inclination-flip homoclinic orbit with $\mu < 1$, $\mu < 2\nu$ using Lin's methods [16]. Recently, the existence of Hénon-like strange attractors was proved in [22], using a result of Mora and Viana [20], in the case where $1 < \mu + \nu$, $\nu < \frac{1}{2}$, $\mu > K\nu$ with some large enough K. See also [21] and [13] for relevant results.

With regards to the orbit-flip homoclinic orbits, Sandstede [25] has proven that homoclinic doubling and homoclinic N-tupling bifurcations ($N \geq 3$) as well as the shift dynamics do occur in its unfolding. There is also a numerical simulation done by [10] for piecewise-linear vector fields involving an orbit-flip homoclinic orbit which shows interesting bifurcation curves for N-homoclinic orbits with $2 \leq N \leq 11$. Our work was inspired by this last result.

Here we state a theorem concerning the homoclinic doubling bifurcations for homoclinic orbits of inclination-flip or orbit-flip type. Consider the family of vector fields X_η with a hyperbolic equilibrium point O. This theorem summarizes some results from [12] and [25].

Theorem 2.3. *Let X_η be a generic two-parameter family of vector fields which has either an orbit-flip or an inclination-flip homoclinic orbit Γ at $\eta = 0$. Then the following holds:*

(1) If $1 < \nu = \frac{\lambda_s}{\lambda_u}$, the homoclinic doubling bifurcation does not occur.

(2) If $\frac{1}{2} < \nu < 1$ and $\mu = \frac{\lambda_{ss}}{\lambda_u} > 1$, the homoclinic doubling bifurcation occurs. More precisely, there exists a local change of parameters at $\eta = 0$

$$\varepsilon = (\varepsilon_1, \varepsilon_2) = \varepsilon(\eta),$$

and curves of the form

$$\varepsilon_2 = \kappa_{2H}(\varepsilon_1) \quad (\varepsilon_1 \geq 0),$$

$$\varepsilon_2 = \kappa_{PD}(\varepsilon_1) \quad (\varepsilon_1 \geq 0),$$

$$\varepsilon_2 = \kappa_{SN}(\varepsilon_1) \quad (\varepsilon_1 \leq 0),$$

in the parameter space such that a primary homoclinic orbit persists along $\varepsilon_2 = 0$ *whereas a doubled homoclinic orbit bifurcates along* $\varepsilon_2 = \kappa_{2H}(\varepsilon_1)$, *a periodic orbit undergoes the period doubling bifurcation along* $\varepsilon_2 = \kappa_{PD}(\varepsilon_1)$, *and the saddle-node bifurcation occurs for periodic orbits along* $\varepsilon_2 = \kappa_{SN}(\varepsilon_1)$. *Moreover,*

$$\kappa_{2H}(\varepsilon_1) \approx \varepsilon_1^{\frac{1}{1-\nu}},$$

$$\kappa_{PD}(\varepsilon_1) \approx c\varepsilon_1^{\frac{1}{1-\nu}} \text{ for some } 0 < c < 1,$$

$$\kappa_{SN}(\varepsilon_1) \approx c'|\varepsilon_1|^{\frac{1}{1-\nu}} \text{ for some } c' < 0.$$

See also [17] and references therein for more information.

Next we shall derive a two-parameter family of one-dimensional maps in order to study the dynamics and bifurcations that occur in an unfolding of orbit-flip homoclinic orbits. This family is obtained by taking the singular limit of the two-dimensional return maps along the homoclinic orbit as the strong stable eigenvalue going to $-\infty$.

Let X_η be the generic two-parameter unfolding as above which possesses an orbit-flip homoclinic orbit Γ to a hyperbolic equilibrium point O at $\eta = 0$. Γ lies in the intersection of the unstable and strong stable manifolds $W^u(O) \cap W^{ss}(O)$. We choose the (x, y, z)-coordinates in such a way that the local stable, unstable and strong stable manifolds are given by

$$W_{loc}^u(O) = \{x = y = 0\}, \quad W_{loc}^s(O) = \{z = 0\}, \quad W_{loc}^{ss}(O) = \{x = z = 0\}$$

in a neighborhood of O. We assume for simplicity that the vector fields X_η are uniformly smoothly linearizable in a neighborhood of O containing the unit cube $[-1, 1]^3$, and take the two cross sections

$$\Sigma^0 = \{y = 1\}, \quad \Sigma^1 = \{z = 1\}$$

which are transverse to the homoclinic orbit Γ. Then the Poincaré map for X_η along Γ will be given by composition of the following two mappings:

$$\text{the local map}: \quad \Sigma^0 \to \Sigma^1 \quad ; \quad \begin{pmatrix} x \\ 1 \\ z \end{pmatrix} \mapsto \begin{pmatrix} xz^\nu \\ z^\mu \\ 1 \end{pmatrix},$$

$$\text{the global map}: \quad \Sigma^1 \to \Sigma^0 \quad ; \quad \begin{pmatrix} X \\ Y \\ 1 \end{pmatrix} \mapsto \begin{pmatrix} p + \alpha X + \beta Y + h.o.t. \\ 1 \\ q + \gamma X + \delta Y + h.o.t. \end{pmatrix},$$

where $\mu = \frac{\lambda_{ss}}{\lambda_u}$ and $\nu = \frac{\lambda_s}{\lambda_u}$. Note that the constants, in particular, p and q may depend on the unfolding parameter η. Since the orbit-flip homoclinic orbit exists when $(1, 0, 0)$ is mapped to $(0, 1, 0)$ under the global map, we have

$$p(\eta) = q(\eta) = 0.$$

Therefore the parameter η should be taken in such a way that

$$\left. \frac{\partial(p, q)}{\partial(\eta_1, \eta_2)} \right|_{\eta=0} \neq 0.$$

In other words, (p, q) can be thought of as unfolding parameters, and consequently, the return map h takes the form

$$(x, z) \mapsto \begin{pmatrix} p \\ q \end{pmatrix} + \begin{pmatrix} \alpha & \beta \\ \gamma & \delta \end{pmatrix} \begin{pmatrix} xz^\nu \\ z^\mu \end{pmatrix} + \begin{pmatrix} h.o.t. \\ h.o.t. \end{pmatrix}.$$

Here we consider the case that the strong stable eigenvalue has a very large modulus so that we can neglect the term involving z^μ. Then the most dominant terms in the return map reduce to give a one-dimensional map

$$z \mapsto \alpha(z - q + \frac{\gamma p}{\alpha})z^\nu + q,$$

or, by rescaling the variable and parameters,

$$f(x) = (x - a - b)x^\nu + b.$$

Note that here we have assumed $\alpha > 0$ for simplicity, since the other case can be treated similarly. In the next section we fix ν as being $\frac{1}{2} < \nu < 1$ and consider the bifurcation of this two-parameter family of one-dimensional maps that are related to the dynamics of original vector fields.

3 Analysis of reduced one-dimensional maps

In this section we shall show that the two-parameter family of maps

$$f(x; a, b) = (x - a - b)x^\nu + b \quad \left(\frac{1}{2} < \nu < 1\right)$$

possesses an infinite sequence of special doubling bifurcations that can be interpreted as homoclinic doubling bifurcations of corresponding vector fields. First we note that the orbit of 0 for the one-dimensional map corresponds to the unstable manifold of the equilibrium point for the vector field, and therefore we only consider the maps on the interval $[0, f(0)] = [0, b]$ and trace the orbit of 0 as long as it stays in this interval. This map is in general a unimodal map with a minimum which can be either positive or negative depending on the parameters. In particular, the map with the parameters $(a, b) = (0, 0)$ corresponds to the vector field with an orbit-flip. The curve which can be interpreted as the persistence curve for 1-homoclinic orbit coming out from the orbit-flip point is given by the condition that 0 is a fixed point, namely $f(0) = b = 0$, whereas the bifurcation curve for 2-homoclinic orbit is given by $f^2(0) = f(b) = 0$, hence $a = b^{1-\nu}$. These two bifurcation curves nicely fit with the bifurcation diagram for the vector fields that unfold an orbit-flip.

In general homoclinic orbits for vector fields correspond to periodic orbits through 0 for these one-dimensional maps, which is given by the equation $f^N(0) = 0$. Inclination-flip homoclinic orbits are interpreted as such periodic orbits that pass through 0 and the minimum point, and hence given by the equations $f^N(0) = 0$, $f'(f^{N-1}(0)) = 0$. In particular the inclination-flip 2-homoclinic orbit is given by the equations $f^2(0) = 0$ and $f'(f(0)) = 0$, or equivalently, $(a, b) = (\nu^{\frac{1-\nu}{\nu}}, \nu^{\frac{1}{\nu}})$. It is hard to obtain explicit analytic expressions for the N-homoclinic bifurcation curves with $N > 2$, and hence, we use the following color diagram in order to visualize these curves.

We compute the number

$$m = \min\{n \geq 1 \mid f^n(0; a, b) \leq 0\}$$

and assign a color code for each number m. Then we can draw bifurcation sets with those assigned colors at each parameter value (a, b). Figure 3.1(a) is one example of such color diagrams. Each color code (except black) stands for a rounding number m, for instance, $m = 1$ (blue), 2 (yellowish green), 3 (sky blue), 4 (red), 5 (purple), 6 (yellow) and 7 (white). Higher rounding numbers m not larger than a number called $Maxcount$ are coded as $(m - 1)\mathrm{mod}(7) + 1$. If $m > \mathrm{Maxcount}$ or $m = \infty$, then black is assigned. By definition, each point of the boundary of a region with a specific color satisfies $f^m(0) = 0$ for certain

Figure 3.1: Color-coded homoclinic bifurcation diagram for one-dimensional map $f(x) = (x - a - b)x^\nu + b$ where $\nu = 0.8$. (a) (a,b)-parameter space: $0.0 \le a \le 2.0$, $0.0 \le b \le 5.0$, Maxcount $= 30$. (b) (y_*, x_*)-parameter space: $0.0 \ge y_* \ge -0.1$, $0.0 \le x_* \le 2.0$, Maxcount $= 30$. (c) Successive homoclinic doubling bifurcations. Horizontal axis: $-9.5 \le \log_{10} y_* \le 0.0$, Vertical axis: $\log_{10} b_0 \ge \log_{10}(b_0 - x_*) \ge -8.0$, where $b_0 = 1.151739$ and $\log_{10} b_0 = 0.061354$, Maxcount $= 1024$.

number m, and hence it corresponds to a homoclinic bifurcation point for m-homoclinic orbit. For example, the boundary H_4 of a red region with $m = 4$ exhibits a 4-homoclinic bifurcation curve. In this way, it is quite easy to see the bifurcation curves for N-homoclinic orbits with various N.

It can be seen that there is a curve at the envelop of all colored regions. This is given by the condition that the minimum value of f is equal to 0, since if the minimum value is positive, then the orbit of 0 never becomes negative and hence, by the rule of color assignment, such a parameter value is colored in black. This condition of the envelop is given by $f'(x_*) = 0$, $f(x_*) = 0$, or equivalently,

$$a + b = \frac{1 + \nu}{\nu}(\nu b)^{\frac{1}{1+\nu}}.$$

Using this expression of the envelop, we make the change of parameters from (a, b) to

$$x_* = \frac{\nu}{1 + \nu}(a + b), \quad y_* = f(x_*) = b - \frac{1}{\nu}\left(\frac{\nu}{1 + \nu}(a + b)\right)^{1+\nu}.$$

in such a way that the envelop is mapped to the x_*-axis. Figure 3.1(b) exhibits the color diagram with these new parameters, where we can more easily see the bifurcations, in particular several successive homoclinic doubling bifurcations. This situation can be seen in more detail by taking $(\log x_*, \log y_*)$ as new parameters. See Figure 3.1(c). Observe that the homoclinic doubling bifurcations successively occur from 2-homoclinic orbit to $2^{10} = 1024$-homoclinic orbit.

Since the homoclinic doubling bifurcation in vector fields corresponds to 0 being a periodic orbit that passes through the minimum of the unimodal map f, we shall rigorously show that there exists an infinite sequence of such successive doubling bifurcations in the family of unimodal maps.

	$\nu = 0.501$	$\nu = 0.60$	$\nu = 0.70$	$\nu = 0.80$	$\nu = 0.90$	$\nu = 1.00$
$k = 1$	0.251694	0.426827	0.600774	0.756593	0.889525	0.999999
$k = 2$	0.287954	0.593588	0.847700	1.047174	1.198263	1.310702
$k = 3$	0.289910	0.646458	0.920318	1.125175	1.274332	1.381547
$k = 4$	0.290711	0.663550	0.940856	1.145058	1.292127	1.396945
$k = 5$	0.291060	0.669037	0.946594	1.150062	1.296239	1.400253
$k = 6$	0.291214	0.670792	0.948191	1.151317	1.297187	1.400961
$k = 7$	0.291281	0.671353	0.948635	1.151632	1.297405	1.401113
$k = 8$	0.291311	0.671532	0.948758	1.151711	1.297455	1.401146
$k = 9$	0.291325	0.671590	0.948792	1.151730	1.297467	1.401153
$k = 10$	0.291330	0.671608	0.948802	1.151735	1.297469	1.401154
δ	2.259316	3.131465	3.598464	3.990066	4.342408	4.669195

Table 3.1: Successive homoclinic doublings and the Feigenbaum constant. For each value of ν, the parameter values x_* for inclination-flip 2^k-homoclinic orbits are shown, together with approximate values of the corresponding Feigenbaum constant δ computed from those data.

Theorem 3.1. *The two-parameter family of one-dimensional unimodal maps $f_{a,b}$ has a cascade of doubling bifurcations that can be interpreted as cascade of homoclinic doublings in the above sense.*

Proof. We have only to consider the case where the minimum value of the unimodal map is 0. This will reduce the two-parameter family of unimodal maps to that with only one parameter:

$$\tilde{f}_b = \left\{ x - \frac{1+\nu}{\nu} (\nu b)^{\frac{1}{1+\nu}} \right\} x^\nu + b,$$

since the condition that the minimum is equal to 0 is given by

$$y_* = b - \frac{1}{\nu} \left(\frac{\nu}{1+\nu}(a + b) \right)^{1+\nu} = 0.$$

The family $\tilde{f}_b$ is a C^1-family of unimodal maps that are continuous and onto over the interval $[0, b]$ and of C^1 on $(0, b]$. Therefore this is almost what is called the full family in the sense of Collet-Eckmann, for which the intermediate value theorem for kneading sequences holds. See [2], in particular Theorem III.1.1 for the detail. We can apply this theorem to our family by modifying the proof of Theorem III.1.1 in [2], or more simply by looking at the second iterate $\tilde{f}_b^2$ as

follows: Since we assume the exponent ν satisfying $\frac{1}{2} < \nu < 1$, it is easy to see that $\tilde{f}_b^2$ restricted to $[x_0, b]$ is exactly a full family of C^1-unimodal maps without any singularity, where x_0 stands for the unique fixed point for $\tilde{f}_b$. Since we have computed the existence of the first doubling bifurcation point, we conclude that the cascade of doubling bifurcations occurring in $\tilde{f}_b^2$ gives the desired sequence.

We have numerically computed the Feigenbaum constants for the doubling bifurcations in the family $\tilde{f}_b$ with various exponent ν. It should be noted that when $\nu = 1$, the Feigenbaum constant is close to the standard value 4.6692..., but it is not, when $\frac{1}{2} < \nu < 1$. Our data for the Feigenbaum constants resemble to similar data for the unimodal maps $x \mapsto 1 - a|x|^\zeta$ with $1 < \zeta < 12$ computed in [9] where the exponent ζ corresponds to 2ν in our case.

4 Successive homoclinic doublings in PL vector fields

4.1 Normal forms of three-dimensional two-region proper piecewise-linear vector fields

We shall first summarize results for normal forms of three-dimensional proper two-region piecewise-linear vector fields. Since the proper condition which will be defined later is generic, they form an important class in the study of bifurcations for continuous piecewise-linear vector fields. In particular it can be shown that normal forms of proper systems are determined by elementary symmetric polynomial of eigenvalues in each linear region as described below.

Given a non-zero vector $\alpha \in \mathbb{R}^3$, define a plane

$$V = \{x \in \mathbb{R}^3 | \langle \alpha, x \rangle = 1\}$$

(where $\langle \cdot, \cdot \rangle$ denotes the usual inner product) and half spaces

$$R_\pm = \{x \in \mathbb{R}^3 | \pm (\langle \alpha, x \rangle - 1) > 0\}.$$

Consider a vector field defined by an ordinary differential equation

$$\frac{dx}{dt} = X(x) = \begin{cases} Ax, & (x \in R_-) \\ Bx - p, & (x \in R_+), \end{cases} \tag{4.1}$$

where A and B are 3×3 matrices, and $p \in \mathbb{R}^3$ (all elements of $\mathbb{R}^3$ are column vectors, unless otherwise stated). We call the vector field a *three-dimensional two-region piecewise-linear vector field*, and the plane V the *boundary* of the vector field. This vector field is continuous on the boundary V if and only if

$$B = A + p\alpha^T.$$

See [17, Lemma 2.5.1].

Definition 4.1. Two vector fields X and X' on $\mathbb{R}^3$ are *linearly conjugate* if there is a non-singular matrix $H \in GL(3, \mathbb{R})$ such that

$$HX(x) = X'(Hx) \quad \text{for all} \quad x \in \mathbb{R}^3.$$

Definition 4.2. A vector field X defined by (4.1) is *proper* if any A-invariant proper linear subspace $E \subset \mathbb{R}^3$ intersects with the boundary V, i.e.,

$$A(E) \subset E \quad \text{and} \quad 0 < \dim(E) < 3 \Longrightarrow E \cap V \neq \emptyset. \tag{4.2}$$

Theorem 4.3.

Any proper continuous three-dimensional two-region piecewise-linear vector field given by

$$X'(x) = A'x + \frac{1}{2}p'\{|\langle \alpha', x \rangle - 1| + (\langle \alpha', x \rangle - 1)\}$$

$$= \begin{cases} A'x, & (\langle \alpha', x \rangle - 1 \leq 0) \\ B'x - p', & (\langle \alpha', x \rangle - 1 \geq 0), \end{cases}$$

is linearly conjugate to the vector field defined by

$$X(x) = Ax + \frac{1}{2}p\{|\langle \alpha, x \rangle - 1| + (\langle \alpha, x \rangle - 1)\},$$

$$= \begin{cases} Ax, & (\langle \alpha, x \rangle - 1 \leq 0) \\ Bx - p, & (\langle \alpha, x \rangle - 1 \geq 0), \end{cases}$$

where

$$\alpha = (1, 0, 0)^T, \quad p = (c_1, c_2, c_3)^T,$$

$$A = \begin{pmatrix} 0 & 1 & 0 \\ 0 & 0 & 1 \\ a_3 & a_2 & a_1 \end{pmatrix}, \quad B = \begin{pmatrix} c_1 & 1 & 0 \\ c_2 & 0 & 1 \\ c_3 + a_3 & a_2 & a_1 \end{pmatrix} = A + p\alpha^T$$

$$a_1 = \lambda_1 + \lambda_2 + \lambda_3, \quad a_2 = -(\lambda_1\lambda_2 + \lambda_2\lambda_3 + \lambda_3\lambda_1), \quad a_3 = \lambda_1\lambda_2\lambda_3,$$

$$b_1 = \nu_1 + \nu_2 + \nu_3, \quad b_2 = -(\nu_1\nu_2 + \nu_2\nu_3 + \nu_3\nu_1), \quad b_3 = \nu_1\nu_2\nu_3,$$

$$c_1 = b_1 - a_1, \quad c_2 = b_2 - a_2 + c_1a_1, \quad c_3 = b_3 - a_3 + a_2c_1 + a_1c_2,$$

$\lambda_1, \lambda_2, \lambda_3$ *being the eigenvalues of A and ν_1, ν_2, ν_3 being those of B.*
Moreover, when $\det(B) = b_3 \neq 0$, we can write

$$X(x) = \begin{cases} Ax, & (\langle \alpha, x \rangle - 1 \leq 0) \\ B(x - P), & (\langle \alpha, x \rangle - 1 \geq 0), \end{cases}$$

where

$$P = \left(1 - \frac{a_3}{b_3}, \frac{c_1 a_3}{b_3}, \frac{c_2 a_3}{b_3}\right).$$

See [17, Subsection 2.5.1] for the proof of this theorem.

The vector field X is determined by $\rho = (a_1, a_2, a_3, b_1, b_2, b_3) \in \mathbb{R}^6$, which will be called the *eigenvalue parameters.* Define the boundary V by

$$V = \{x \in \mathbb{R}^3 | \langle \alpha, x \rangle = 1\},$$

and set

$$V_{\pm} = \{x \in V | \pm \langle \alpha, Ax \rangle > 0\}.$$

If λ_i ($i = 1, 2, 3$) is real, then the vector $\overrightarrow{OC_i}$ gives an eigenvector of A associated with λ_i, where

$$C_i = (1, \lambda_i, \lambda_i^2)^T \in V. \tag{4.3}$$

Assume λ_1 and λ_2 are negative real and λ_3 is positive real, whereas ν_1 and ν_2 are a pair of complex-conjugate numbers and ν_3 is real. Denote

$$\nu_1, \nu_2 = \sigma \pm \omega\sqrt{-1}, \quad \nu_3 = \gamma.$$

Since an eigenvector for λ_i is given by (4.3), the one-dimensional unstable eigenspace $E^u(O)$ and the two-dimensional stable eigenspace $E^s(O)$ for $O = (0, 0, 0)^T$ are given by

$$E^u(O) = \{x \in \mathbb{R}^3 | x = r(1, \lambda_3, \lambda_3^2)^T, \langle \alpha, x \rangle - 1 \leq 0, r \in \mathbb{R}\},$$

$$E^s(O) = \{x \in \mathbb{R}^3 | \langle u, x \rangle = 0, \langle \alpha, x \rangle - 1 \leq 0\},$$

where $u = (-1, \frac{\lambda_1 + \lambda_2}{\lambda_1 \lambda_2}, -\frac{1}{\lambda_1 \lambda_2})$. The intersection $E^s(O) \cap V$ is thus given by

$$E^s(O) \cap V = \{x = (x^1, x^2, x^3) \in \mathbb{R}^3 | \langle u, x \rangle = 0, x^1 = 1\}. \tag{4.4}$$

If $\lambda_2 < \lambda_1 < 0$, the strong stable eigenspace $E^{ss}(O)$ is given by

$$E^{ss}(O) = \{x \in \mathbb{R}^3 | x = r(1, \lambda_2, \lambda_2^2)^T, \langle \alpha, x \rangle - 1 \leq 0, r \in \mathbb{R}\}.$$

Take a point $C_3 = (1, \lambda_3, \lambda_3^2)^T \in V_+$ on the local unstable manifold of O and consider its entire orbit $\mathcal{O}(C_3)$. The integer $m > 0$ is called the *rounding number* of the orbit if

$$m = \frac{1}{2}\sharp(\mathcal{O}(C_3) \cap V).$$

Figure 4.1: Color-coded homoclinic bifurcation diagram for three-dimensional continuous piecewise-linear vector field with $\lambda_1 = -0.2, \lambda_2 = -0.4, \lambda_3 = 0.3, \omega = 1.0$. (a) Horizontal axis: $0.0 \geq \gamma \geq -0.26$, Vertical axis: $0.0 \leq \sigma \leq 0.3$, Maxcount $= 20$. (b) Enlargement of (a). Horizontal axis: $0.0 \geq \gamma \geq -0.26$, Vertical axis: $0.1 \geq H_1(\gamma) - \sigma \geq 0.0$, where $\sigma = H_1(\gamma)$ is a function which gives the 1-homoclinic bifurcation curve H_1 in (a). Maxcount $= 20$. (c) Enlargement of (b). Horizontal axis: $0.0 \geq \gamma \geq -0.16$, Vertical axis: $0.01 \geq H_2(\gamma) - \sigma \geq 0.0$, where $\sigma = H_2(\gamma)$ is a function which gives the 2-homoclinic bifurcation curve H_2 in (b). Maxcount $= 20$. (d) Enlargement of (c). Horizontal axis: $0.0 \geq \gamma \geq -0.08$, Vertical axis: $0.001 \geq H_4(\gamma) - \sigma \geq 0.0$, where $\sigma = H_4(\gamma)$ is a function which gives the 4-homoclinic bifurcation curve H_4 in (c). Maxcount $= 20$. (e) Successive enlargements of a line segment in (d) with $\gamma = -0.074$ fixed, Maxcount $= 128$. Left: $0.1537311 \leq \sigma \leq 0.1537811$, that corresponds to $0.00010 \geq H_4(\gamma) - \sigma \geq 0.00015$. Middle: $0.1537433 \leq \sigma \leq 0.1537437$. Right:$0.1537433998075 \leq \sigma \leq 0.1537433998125$.

4.2 Successive homoclinic doublings in piecewise-linear vector fields

We take a piecewise-linear vector field with an orbit-flip, put it into the normal form using Theorem 4.3 and regard the eigenvalues as parameters that unfold the orbit-flip homoclinic obit. Figure 4.1(a) exhibits bifurcations in the normal form family. This figure is produced as a color diagram, namely we start the point C_3 in one branch of the local unstable manifold and count the rounding number m defined in the previous subsection. Each color code (except black) stands for a rounding number m in the same way as before, namely, $m = 1$ (blue), 2 (yellowish green), 3 (sky blue), 4 (red), 5 (purple), 6 (yellow) and 7 (white) and higher rounding numbers $m \leq$ Maxcount are coded as $(m - 1)\mathrm{mod}(7) + 1$. If $m >$ Maxcount or $m = \infty$, black is assigned. The assignment of color codes changes only when either the orbit hits the stable manifold or it becomes tangent to the boundary of the linear region, the latter case of which is not observed in our numerical experiments. Therefore the boundary of a colored region corresponds to a bifurcation curve for some homoclinic orbits. In this figure, we can see, among other things, the boundary H_1 of blue region with $m = 1$ which corresponds to the 1-homoclinic bifurcation curve.

Figures 4.1(b) - 4.1(d) are successive enlargements of Figure 4.1(a). In Figure 4.1(b), we can see a 2-homoclinic bifurcation curve as the boundary H_2 of

yellowish green region with $m = 2$, and in Figure 4.1(c), a 4-homoclinic bifurcation curve as the boundary H_4 of red region with $m = 4$. Figure 4.1(d) is yet another enlargement where a 8-homoclinic bifurcation curve can be observed. These homoclinic bifurcation curves are computed by using the bifurcation equation given in [17, Subsection 2.5.4]. Moreover, it is also possible to compute the inclination-flip bifurcation points from these bifurcation equations. Since it is not easy to keep following such homoclinic bifurcations curves by enlargements of two-dimensional parameter space, we instead fix a line segment in the parameter space that cuts through the region where successive homoclinic doubling bifurcations are expected to occur. Enlargements of the bifurcation diagram along the line segment is much easier to carry out, as seen in Figure 4.1(e), where successive homoclinic doubling bifurcation sets for up to $2^6 = 64$-homoclinic orbits are observed. A 2^N-homoclinic bifurcation set with higher N is not seen, because the width of the corresponding colored region shrinks extremely fast so that it quickly exceeds the computational limit. However, this kind of computational difficulty on a fixed line segment is also observed in the similar computation for one-dimensional maps done in Section 3, and since we found successive homoclinic doublings for one-dimensional maps along the special curve given as the envelop of the colored region, we can similarly expect that cascade of homoclinic doubling bifurcations do occur for this family of piecewise-linear vector fields as well.

References

[1] S.-N. Chow, B. Deng and B. Fiedler, Homoclinic bifurcation at resonant eigenvalues, *J. Dynam. Diff. Eq.* **2** (1990) 177–244.

[2] P. Collet and J.-P. Eckmann, *Iterated Maps of the Interval as Dynamical Systems*, 1980, Birkhäuser.

[3] B. Deng, The Sil'nikov problem, exponential expansion, strong λ-lemma, C^1-linearization, and homoclinic bifurcation, *J. Diff. Eq.* **79** (1989) 189–231.

[4] B. Deng, Homoclinic twisting bifurcations and cusp horseshoe maps, *J. Dynam. Diff. Eq.* (1993) 417–467.

[5] J. W. Evans, N. Fenichel and J. A. Feroe, Double impulse solutions in nerve axon equations, *SIAM J. Appl. Math.* **42** (1982) 219–234.

[6] M. Feigenbaum, Quantitative universality for a class of nonlinear transformations, *J. Stat. Phys.* **19** (1978) 25–52; *ibid.* **21** (1979) 669–709.

[7] A. J. Homburg, H. Kokubu and M. Krupa, The cusp horse-shoe and its bifurcations in the unfolding of an inclination-flip homoclinic orbit, *Ergod. Th. Dynam. Sys.* **14** (1994) 667–693.

[8] M. Hirsch, C. Pugh and M. Shub, *Invariant Manifolds*, Lect. Notes in Math., Vol. 583, 1977, Springer.

[9] B. Hu and I. I. Satija, A spectrum of universality classes in period doubling and period tripling, *Phys. Lett. A.* **98** (1983) 143–146.

[10] K. Iori, E. Yanagida, and T. Matsumoto, N-homoclinic bifurcations of piecewise-linear vector fields, in *Structure and Bifurcations of Dynamical Systems* (Ed. S. Ushiki), Advanced Series in Dynamical Systems, Vol. 11, 1993, pp. 82–97, World Scientific.

[11] M. Kisaka, H. Kokubu and H. Oka, Supplement to homoclinic doubling bifurcation in vector fields, in *Dynamical Systems* (Eds. R. Bamon, R. Labarca, J. Lewowicz and J. Palis, Jr), Pitman Research Notes in Math., Vol. 285, 1993, pp. 92–116, Longman Scientific & Technical.

[12] M. Kisaka, H. Kokubu and H. Oka, Bifurcations to N-homoclinic orbits and N-periodic orbits in vector fields, *J. Dynam. Diff. Eq.* **5** (1993) 305–357.

[13] H. Kokubu and V. Naudot, Existence of infinitely many homoclinic doubling bifurcations from some codimension three homoclinic orbits, preprint.

[14] M. Komuro, Normal forms of continuous piecewise-linear vector fields and chaotic attractors, Part I, *Japan J. Appl. Math.* **5** (1988) 257–304; Part II, *ibid.* **5** (1988) 503–549.

[15] M. Komuro, Bifurcation equations of continuous piecewise-linear vector fields, *Japan J. Ind. Appl. Math.* **9** (1992) 269–312.

[16] X.-B. Lin, Using Melnikov's method to solve Silnikov problems, *Proc. Royal Soc. Edinburgh* **116A** (1990) 295–325.

[17] T. Matsumoto, M. Komuro, H. Kokubu, and R. Tokunaga, *Bifurcations – Sights, Sounds, and Mathematics*, 1993, Springer.

[18] W. de Melo and S. van Strien, *One-Dimensional Dynamics*, 1993, Springer.

[19] J. Milnor and W. Thurston, On iterated maps of the interval, in *Dynamical Systems*, Lect. Notes Math., Vol. 1342, 1988, pp. 465–563, Springer; the original preprint, 1977, Princeton.

[20] L. Mora and M. Viana, Abundance of strange attractors, *Acta Math.* **171** (1993) 1–71.

[21] V. Naudot, Hyperbolic dynamics in the unfolding of a degenerate homoclinic orbit, preprint, 1994.

[22] V. Naudot, Strange attractor in the unfolding of an inclination-flip homoclinic orbit, to appear in *Ergod. Th. Dynam. Sys.*

[23] S. Nii, N-homoclinic bifurcations for homoclinic orbits changing its twisting, preprint Kyoto-Math 94-20.

[24] M. R. Rychlik, Lorenz-attractors through Šil'nikov-type bifurcation, Part I, *Ergod. Th. Dynam. Sys.* **10** (1990) 793–821.

[25] B. Sandstede, Verzweigungstheorie homokliner Verdopplungen, Ph. D. thesis, University of Stuttgart, 1993.

[26] B. Sandstede, in preparation.

[27] E. Yanagida, Branching of double pulse solutions from single pulse solutions in nerve axon equations, *J. Diff. Eq.* **66** (1987) 243–262.
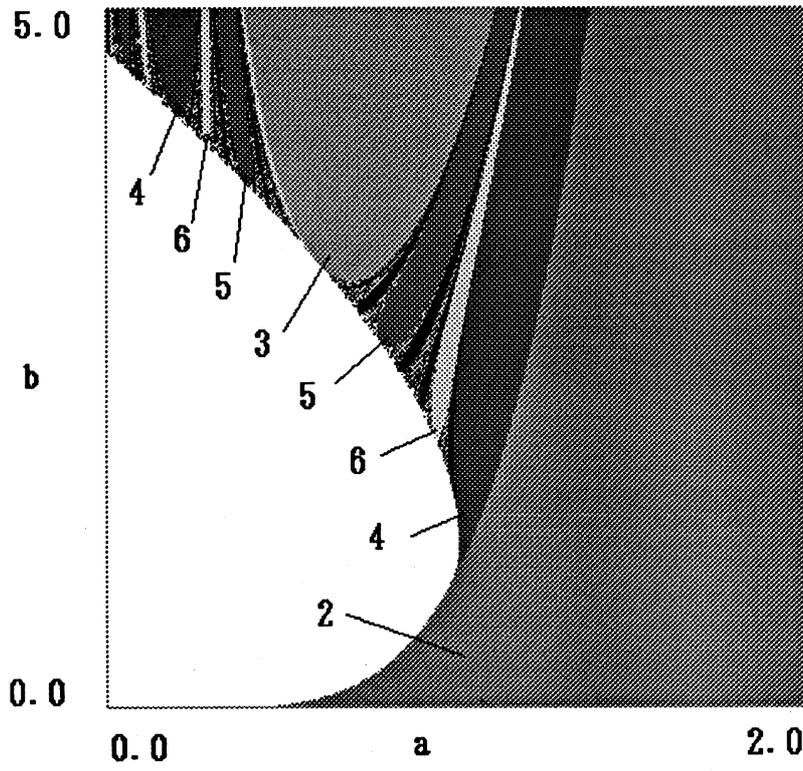
Fig 3.1(a)
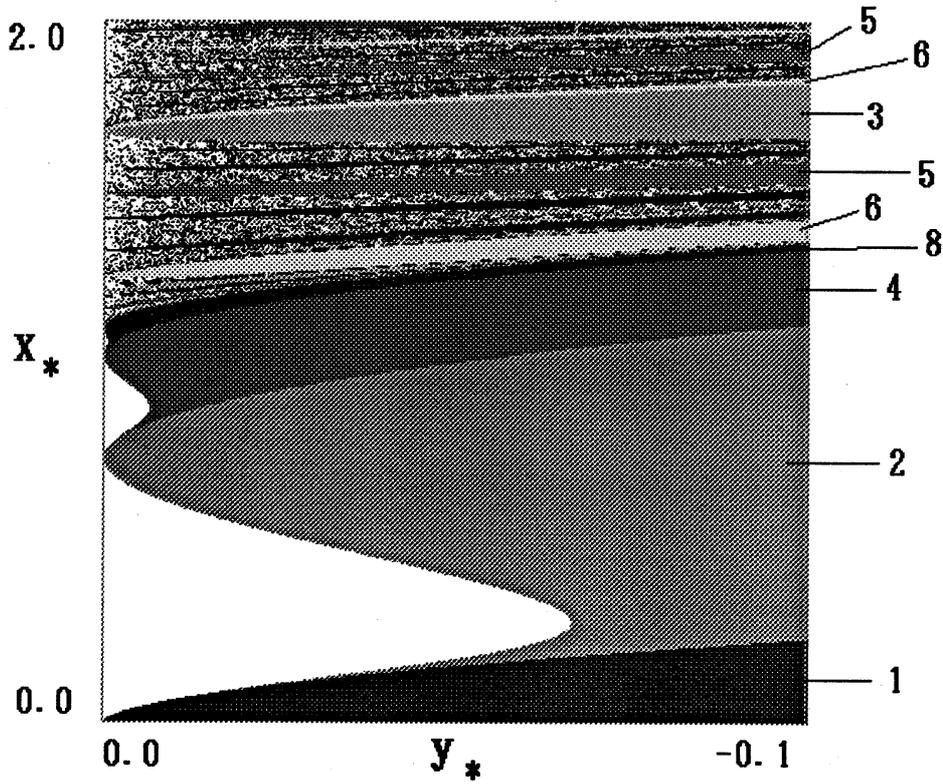
Fig 3.1(b)
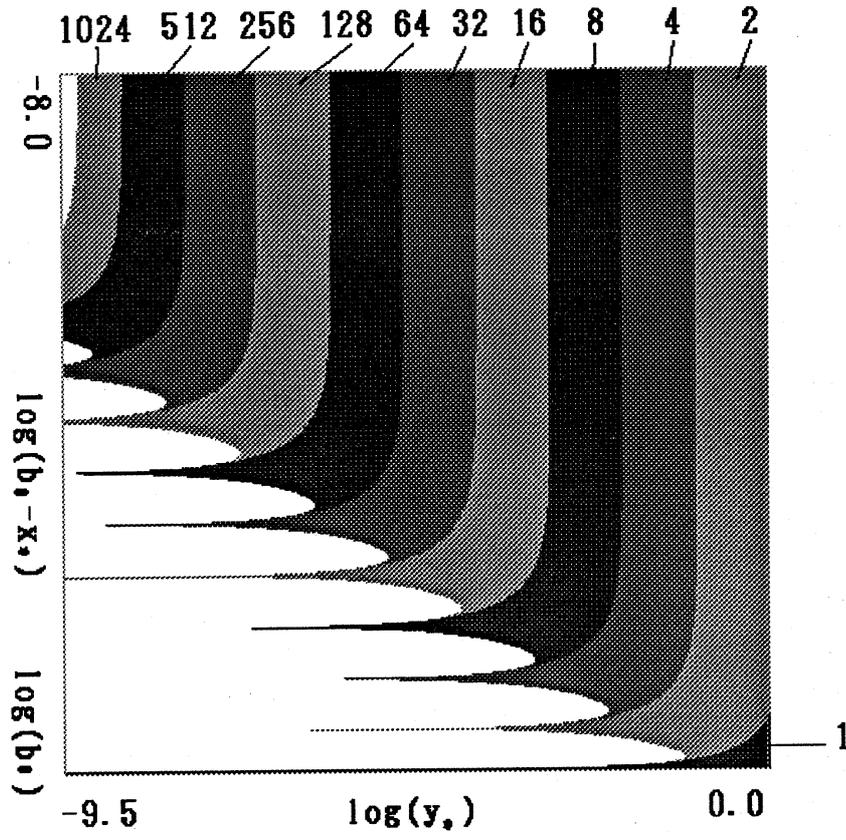
Fig 3.1(c)
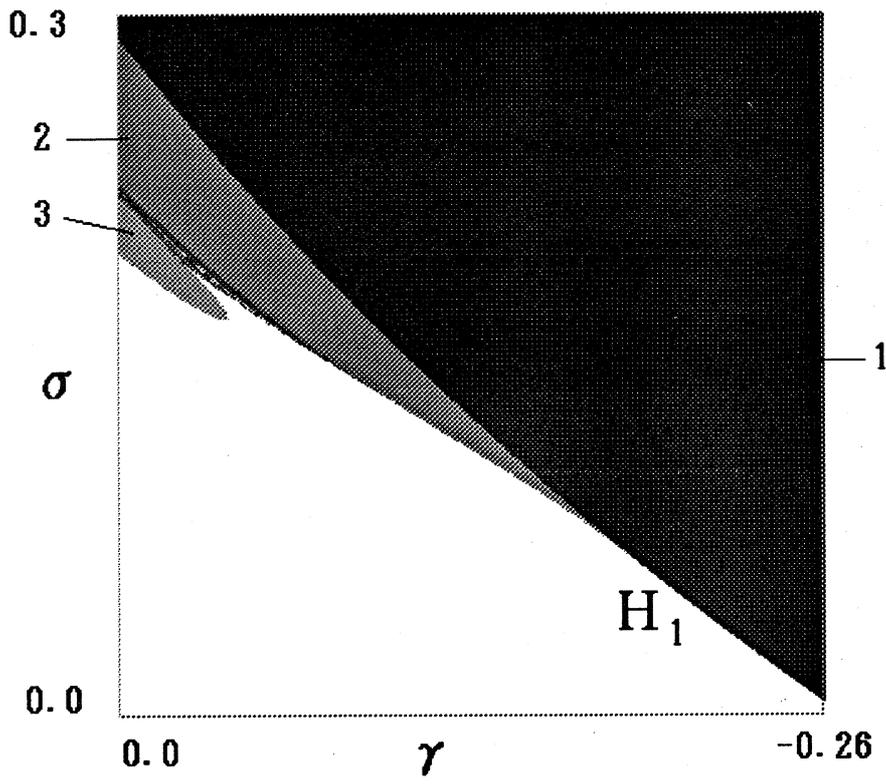
Fig 4.1(a)
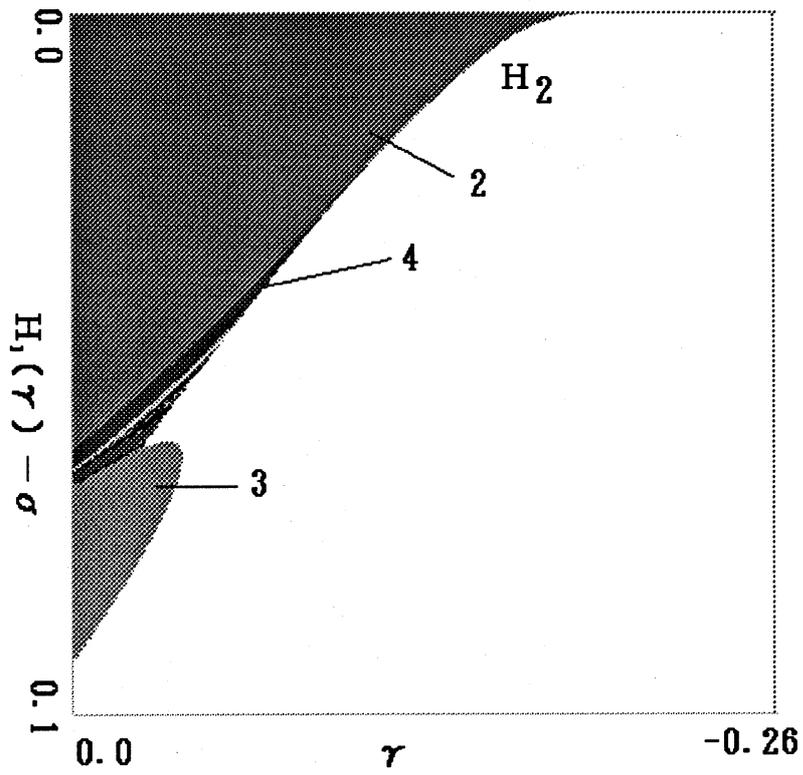
Fig 4.1(b)

Fig 4.1(c)

Fig 4.1(d)

Fig 4.1(e)